ELSEVIER

International Journal of Pharmaceutics 157 (1997) 93–102

international journal of pharmaceutics

Growth mechanisms of high-shear pelletisation

P. Vonk [a,*], C.P.F. Guillaume [a], J.S. Ramaker [a], H. Vromans [b], N.W.F. Kossen [a]

[a] *Department of Pharmaceutical Technology and Biopharmacy, Ant. Deusinglaan 1, 9713 AV, Groningen, The Netherlands*
[b] *Department of Pharmaceutics, Organon International, Oss, The Netherlands*

Received 16 April 1997; received in revised form 7 July 1997; accepted 21 July 1997

Abstract

Two high-shear mixers, Gral 10 and Gral 25, were used to prepare pellets of microcrystalline cellulose and lactose, using water as binder liquid. Growth of pellets was investigated by measuring the pellet size distribution during the process. On the basis of the experiments the destructive nucleation growth mechanism was defined. Pelletisation was started with the formation of large primary nuclei. Small secondary nuclei were formed due to break-up of the primary nuclei. This nucleation process could be described by the comparison of the theoretical tensile strength of the nuclei and the dynamic impact pressure. Due to densification, the secondary nuclei became stronger and growth proceeded exponentially by coalescence. During the kneading stage, net growth was diminished until a steady state was observed. The mean pellet size did not change during the final stage of the kneading phase which resulted in a well-defined product. © 1997 Elsevier Science B.V.

Keywords: Pelletisation; High-shear mixer; Growth mechanism; Nucleation; Kinetics

1. Introduction

Pelletisation is a process in which spherical pellets are formed with a particle size between 300 and 1500 μm. Pelletisation has been achieved in a large variety of equipment: pan and drum mixers, medium and high-shear mixers, roller presses, rotary processors, and extruders. In this study, two high-shear mixers (Collette Gral 10 and Collette Gral 25) were used for the preparation of pellets.

Growth of granules and pellets, which occurs during the liquid addition stage and the kneading stage, has been studied to a large extent (Adetayo et al., 1995; Hancock et al., 1992; Kapur and Fuerstenau, 1966; Knight, 1993; Kristensen and Schæfer, 1995; Ouchiyama and Tanaka, 1975; Schæfer et al., 1992). Usually drum and pan granulation have been investigated. These theories of the mechanisms of growth can not be translated directly to high-shear pelletisation, because the physical circumstances are quite different due to the high-shear forces present.

* Corresponding author. E-mail: p.vonk@farm.rug.nl

PII S0378-5173(97)00232-9

Investigation of the process under different circumstances by changing the process variables results in a better understanding of the mechanisms of growth during the pelletisation process. Many authors described the influence of the liquid content and the process time on granule growth (Adetayo et al., 1993; Holm et al., 1985; Holm, 1996; Newton et al., 1995; Vertommen and Kinget, 1996). These studies were often restricted to the removal of fines, the pellet growth during the kneading phase, and optimisation of the process by factorial design. So far precise understanding of the underlying mechanisms and subsequent control of the process are still a topic of great interest (Ennis, 1996).

The mechanisms of growth have been described previously by Sastry and Fürstenau (1977), and divided into three stages: nucleation, growth by coalescence and layering, and break-up. Schæfer and Mathiesen (1996) described two nucleation mechanisms for melt pelletisation, i.e. immersion and distribution, depending on the ratio between the particle size and the binder droplet size. Hoornaert et al. (1994) described the nucleation of particles due to collisions between particles with a wetted surface. Here, firstly the wetting of the particles occurs and secondly the collision between the wetted particles. After the nuclei are formed (in most studies, nuclei are already formed, because of the moistened feed materials used in these experiments), growth by coalescence and layering takes place. Coalescence of particles is characterised by the exponential growth of the mean particle size. During coalescence, pellets become more dense by the impact of the impeller and rounded by the collisions with the wall of the bowl and with other pellets. Also break-up of pellets occur when pellets hit the impeller and the chopper.

1.1. Aim

The aim of this study is to investigate nucleation and growth of agglomerates during the liquid addition and kneading phase of the pelletisation process in a high-shear mixer.

2. Materials and methods

2.1. Materials

Microcrystalline cellulose (Avicel PH101, FMC, Wallingstown, Ireland, density 1608 kg/m^3) and lactose 200 mesh (DMV, Veghel, The Netherlands, density 1540 kg/m^3) were used as starting materials. The geometric-weight mean diameter, d_{gw}, of Avicel PH101 is 63 μm and of lactose 200 mesh is 45 μm. Pure water was used as binder liquid (surface tension 0.072 N/m).

2.2. Equipment

Two commercially available vertical high-shear mixers, Gral 10 and Gral 25, (Machines Collette, Wommelgem, Belgium) were used for the preparation of pellets. The impeller speed in the Gral 25 was continuously adjustable (from 2 to 499 rpm). In the Gral 10, the impeller speed could only be set at two levels (430 and 650 rpm). The chopper speed of both mixers could be set at 0, 1500, and 3000 rpm. The Gral 25 was equipped with a power consumption meter, measuring the power consumption of the impeller motor.

The particle size distribution of the original powder and the pellets was measured by means of laser diffraction analysis using a Malvern 2600 laser diffraction apparatus using an 18 mm beam expander, a 1000 mm lens, and a dry powder feeder. The intragranular porosity was measured by a Autopore II (9220 v3.00) mercury porosimeter.

2.3. Methods

To study the different mechanisms of pelletisation in high-shear mixers, three different experiments were performed.

The first set of experiments examined the growth of the pellets during the pelletisation of equal amounts of Avicel and lactose with water. Table 1 gives the exact amounts of material used. The liquid addition rate was set to 82 g/min by means of a peristaltic pump (type 5040, Watson Marlow) and supplied by a nozzle (type 2, BLM 9 60, Delevan 1/8). When the droplet size is esti-

mated on the basis of a comparison between the gravity force and capillary force a value of 4.7 mm is found. The actual droplet size is probably somewhat smaller. During the liquid addition stage the chopper was set to 3000 rpm, and the impeller speed was set to 430 rpm in the Gral 10, and to 276 rpm in the Gral 25 in order to keep the tip velocity constant at 5.2 m/s. In this way dynamic similarity between the two mixers was obtained. After the addition of the binder liquid the wet mass was kneaded for 15 min. During the kneading stage the chopper was switched off. The Gral 10 was also used for an additional experiment where the impeller speed was set to 650 rpm during the kneading stage. The wet pellets were tray-dried for 24 h at 60°C. The growth of the pellets was investigated by measuring the particle size distribution at different processing times during the liquid addition and kneading stage. Each measurement of the particle size distribution was done with a new batch. Because of the closed system used, evaporation ($< 0.5‰$) of liquid does not play a role in the process.

The second set of experiments investigated the formation and growth of nuclei during the liquid addition stage by preparing separate nuclei using indigotine t132 (0.33 kg/m^3) as colouring agent in the binder liquid. The coloured binder liquid was added to the Gral 25 in 2 min (164 gram binder liquid) after which the process was stopped. The impeller speed was set at 15, 50, 100, 150, and 276 rpm in order to investigate the influence of the impeller speed on the break-up of nuclei. The chopper was switched off during these experiments An additional experiment was performed at the highest impeller speed where the chopper speed was set to 3000 rpm. By investigating the distribution of the coloured binder liquid in the bowl directly after the liquid addition, conclusions could be drawn about the nucleation of pellets. It was possible to scale-down the process of nucleation in a packed bed of powder to retrieve more information about the size of a single nucleus. The nuclei in a packed bed were prepared by dropping single droplets with a volume of 0.29 ml on a non-moving bed of particles. After the nuclei were formed, the diameter and mass were measured, and the total volume, porosity and saturation were calculated assuming spherical agglomerates.

A third experiment determined the porosity of the prepared pellets by mercury porosity measurements.

Table 1
Amount of material used during wet pelletisation

Material	Gral 10	Gral 25
Avicel PH101 (kg)	0.4	1.25
Lactose 200 M (kg)	0.4	1.25
Water (kg)	0.43	1.25

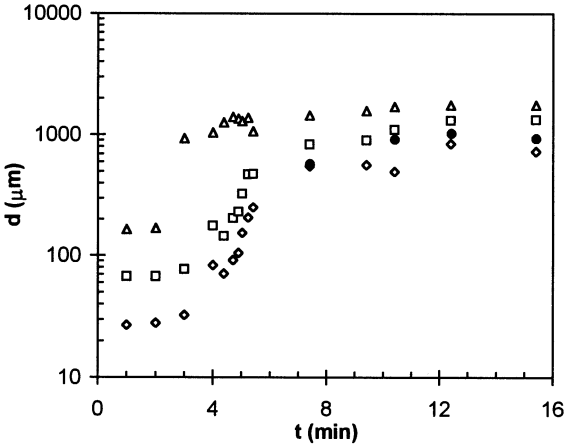

Fig. 1. Growth of pellets in the Gral 10 at an impeller speed of 430 rpm. The diamonds (◇) are the d_{10} data, the rectangles (□) represent the d_{50} data, and the triangles (☆) represent the d_{90} data. The dots (•) represent the d_{50} data of the Gral 10 at an impeller speed of 650 rpm during the kneading stage. Liquid addition time = 5:25 min.

3. Results and discussion

3.1. Growth of pellets

The growth of the pellets was investigated by means of the particle size where 10% (d_{10}), 50% (d_{50}) and 90% (d_{90}) of the volumetric particle size distribution are smaller than the given value. The d_{10}, d_{50}, d_{90} values of the Gral 10 are given in Fig. 1 and the d_{10}, d_{50}, d_{90} values of the Gral 25 are given in Fig. 2. Also given are the d_{50} data of the

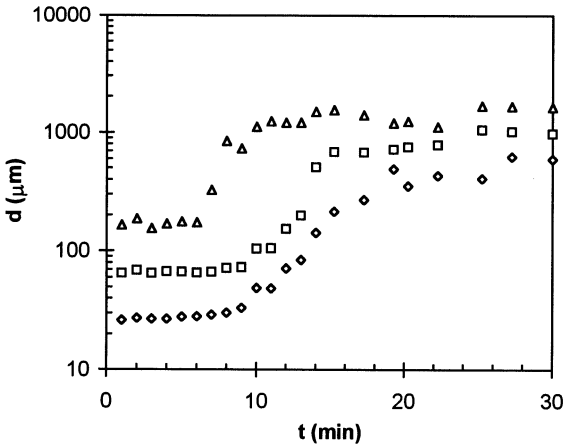

Fig. 2. Growth of pellets in the Gral 25. The diamonds (◇) are the d_{10} data, the rectangles (□) represent the d_{50} data, and the triangles (△) represent the d_{90} data. Liquid addition time = 15:15 min.

Gral 10 while the impeller speed was set to 650 rpm during the kneading stage. The importance of the liquid content can be seen in Fig. 3 which gives the growth curves as a function of the liquid content.

The characteristics of growth of the pellets in both mixers are quite similar. Initially little growth occurs which is demonstrated by the horizontal lines of the growth curves. After the addition of approximately 0.2 gram liquid per gram solid, growth of the largest particles is observed (d_{90}). Growth of the small- and medium- ranged particles (d_{10}, d_{50}) begins after the addition of approximately 0.3 gram liquid per gram solid. Liquid addition is stopped after the addition of 0.5 gram liquid per gram solid in the Gral 25 and after the addition of 0.55 gram liquid per gram solid in the Gral 10.

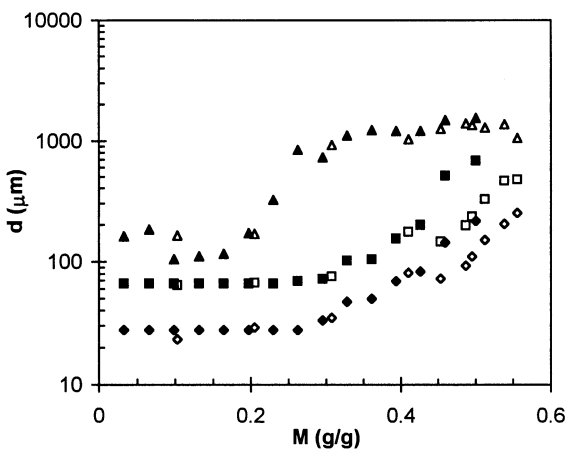

Fig. 3. The growth of pellets as a function of the liquid contents. The diamonds (◇) are the d_{10} data, the rectangles (□) represent the d_{50} data, and the triangles (△) represent the d_{90} data. The open symbols represent the data of the Gral 10 and the closed symbols represent the data of the Gral 25.

The beginning of growth in the Gral 10 seemed to be somewhat delayed. This is probably caused by the fact that the relative amount of lumps adhering to the impeller and bowl wall is smaller for the Gral 10. Therefore, relatively more powder is available to sorb liquid.

At the end of the liquid addition stage exponential growth is present and spherical pellets are formed. This is demonstrated in Fig. 1 and Fig. 2 by the straight lines during the growth of the pellets on a logarithmic scale. Exponential growth can be described by (Leuenberger and Imanidis, 1986):

$$\frac{\mathrm{d} \ln d_{50}}{\mathrm{d}t} = k$$

This relation is found in the Gral 10 between 4 and 6 min processing time and in the Gral 25 between 8 and 16 min. The estimated exponential growth coefficient k of the Gral 10 and 25 are 39 s^{-1} and 7.7 s^{-1} respectively. The value of k is a measure of the relative amount of successful collisions occurring in the mixers. The ratio of the two exponential growth coefficients is equal to five. This suggests that the number of successful collisions in the Gral 10 is five times higher than the number of successful collisions in the Gral 25. This is caused by two effects. The specific liquid addition rate, which is given by the flow rate of the liquid divided by the amount of solids present is approximately three times higher in the Gral 10. The impeller speed is approximately 1.5 times higher in the Gral 10. A higher impeller speed increases the rate of mixing and thereby the number of successful collisions. These two mechanisms together explain why the exponential growth coefficient is five times higher in the Gral 10.

After the liquid addition stage, a 15 min period of kneading takes place. Here we see a distinct difference between the two mixers. During the first minutes of the kneading stage, the pellets in the Gral 10 still grow considerably, while growth of pellets in the Gral 25 ceases to exist. This is mainly caused by the different amount of total liquid applied to the powder mass. In the Gral 10, an extra amount of 7.5% binder liquid was added to the powder mass. Due to this additional 7.5% binder liquid the mean pellet size increases with approximately 35%. This also shows the large influence of the liquid content.

Another interesting phenomenon is the fact that the net growth of the pellets seems to have stopped during the final stages of the kneading phase. Usually granulation is stopped while growth is still present (Leuenberger and Imanidis, 1986; Knight, 1993; Schæfer et al., 1993). This requires accurate control of the process because of the danger of overwetting and overgrowing of the pellets. Endpoint determination is less critical in our case and comparable to melt pelletisation (Schæfer and Mathiesen, 1996). The question remains whether or not zero net growth is caused by an equilibrium between the break-up of pellets and the growth of pellets or that growth has stopped. This remains to be investigated.

3.2. Nucleation

The initial stages of the granulation process were investigated by the formation of separate nuclei in packed beds of lactose, Avicel and the equal weight mixture of both solids respectively.

The packed-bed experiments can be used as a small-scale experiment to estimate the physical properties of the primary nuclei which are formed when liquid drops are added to the high-shear mixers. Table 2 gives the physical properties obtained from the packed-bed experiments. Given are the measured liquid volume, total volume, and solid mass. From these data the saturation and porosity of the primary nuclei can be calculated. Lactose forms dense nuclei because the lactose particles have a cubical shape (shape factor = 0.62). The Avicel particles have a rod shape (shape factor = 0.27, (Ek et al., 1994)) which leads to very porous nuclei. Table 2 also gives the expected tensile strength of the nuclei based on the formula of Rumpf for the static tensile strength (Schubert et al., 1990):

Table 2
Physical properties of the primary nuclei prepared from the packed bed

Property	Lactose 200 M	Avicel PH101	Mixture
Liquid volume (ml)	0.29	0.29	0.29
Total volume (ml)	2.41	0.83	1.30
Solid mass (g)	2.36	0.33	0.99
Saturation	0.33	0.46	0.44
Porosity	0.36	0.75	0.51
Tensile strength (kPa)	7.26	1.39	4.41

$$\sigma_f = 8S\left(\frac{1-\epsilon}{\epsilon}\right)\frac{\gamma_l \cos(\theta)}{d_p}$$

Here σ_f is the tensile strength, S the saturation, ϵ the porosity, γ_l the surface tension of the binder liquid, θ the angle of contact between the liquid and the solid, and d_p the mean particle size of the packing. The angle of contact was set to zero. The static tensile strength of the primary nuclei is in the order of several kPa.

The presence of lactose makes the use of the tensile strength formula of Schubert somewhat questionable. Lactose dissolves in the binder liquid, lowers the surface tension, increases the viscosity and influences the agglomerate porosity. However, we think that this effect can neglected because the change in surface tension is less than 10% and the presence of cellulose reduces the effect of lactose dissolution. The cellulose absorbs large amounts of water, lowers the amount of lactose which can dissolve. A strong indication of this can be found when scanning electron microscopic pictures are investigated of the pellets before and after the dissolution of the lactose from the pellets. The lactose crystals are clearly visible while the original structure of the cellulose particles can no longer be recognised.

Table 3
Results of the nuclei formation in the moving bed

Impeller (rpm)	σ_{impact} (kPa)	Description
15	2.44	Large primary nuclei are formed with blue nucleus and white shell.
50	27.1	Large primary nuclei together with large secondary nuclei due to break-up.
100	108	Large primary nuclei together with large secondary nuclei due to break-up.
150	244	Light blue colouring of powder mass and large primary nuclei.
276	825	Light blue colouring of powder mass and some large secondary nuclei.
276	825	Light blue colouring of powder mass with very small secondary nuclei. Chopper at 3000 rpm.

Table 3 gives the results of the nucleation experiments in the moving bed. At a low impeller speed large primary nuclei (5 mm) are formed with a dark blue centre (4 mm) and a white shell, which do not fragment in the mixer. The size of the dark blue centre corresponds with an actual droplet size of 3 mm (porosity = 0.51, as given in Table 2). Large primary nuclei break-up when the impeller speed is 50 rpm or higher. Initially large secondary nuclei (1 mm) are formed, which can be identified by the light-blue colour-pattern. The secondary nuclei decrease in size when the impeller speed increases. At an impeller speed of 276 rpm fragmentation is nearly completed because some large and many small secondary nuclei are found. Fragmentation is completed when the chopper is switched on and only small secondary nuclei are found giving the bowl content a light-blue colouring. Fragmentation has been found by other authors, but they describe fragmentation as a part of the liquid distribution stage (Carstensen et al., 1976; Holm et al., 1983).

We can explain the fragmentation of nuclei by comparing the estimated tensile strength of primary nuclei (packed-bed experiments) with the impact pressure caused by the impact of the impeller with a nucleus. In order to estimate the impact pressure we have to estimate the acceleration of the nucleus on impact. The acceleration (a) is estimated by:

$$a = \frac{\Delta v}{\Delta t} \approx v_{tip} \frac{v_{tip}}{2 \cdot d_p}$$

Better estimations of the acceleration can be found using rigorous mathematical models like the distinct element method (Potapov and Campbell, 1994; Thornton et al., 1996). When the estimated acceleration is used, the impact pressure is given by:

$$\sigma_{impact} = \frac{F}{A} = \frac{ma}{\pi/4\, d_a^2} \approx \frac{1/6\, d_a^3}{1/4\, d_a^2}\, \rho\, \frac{v_{tip}^2}{2d_p} = \frac{1}{3}\frac{d_a}{d_p}\rho_a v_{tip}^2$$

Here σ_{impact} is the impact pressure, F the acceleration force, A the cross-sectional area of the agglomerate, m the mass of the agglomerate, a the acceleration of the agglomerate, d_a the diameter of the agglomerate, d_p the diameter of the primary particles, ρ_a the density of the agglomerate, and v_{tip} the tip velocity. The impact pressure based on an agglomerate size of 5 mm is given in Table 3.

The impact pressure is of the same order of magnitude as the tensile strength (Table 2) when the impeller speed is between 15 and 50 rpm. In this range of impeller speeds break-up of nuclei can be expected, which is confirmed by our observations. When the impeller speed is increased break-up of smaller nuclei takes place and distribution of wetted particles in the mixer bowl proceeds rapidly due to the fast mixing in the Gral (relative swept volume $> 1\ s^{-1}$). The tip velocity of the chopper is twice the tip velocity of the impeller at 276 rpm. This explains the complete break-up of the secondary nuclei due to the chopper.

3.3. Power consumption

Fig. 4 gives the measured power consumption of the Gral 25. A number of different stages can be identified. The first stage lasts from approximately 3 to 8 min, where the power consumption rises steadily up to 170 W. Comparing with Fig. 2

it can be seen that this corresponds with the growth of the largest particles. Between 8 and 12 min the power consumption rises up to 290 W with a large variation in the actual value. Here the growth of the smaller particles starts. Between 12 and 15 min the power consumption is fairly constant, corresponding with the rapid growth of the d_{50} particles. After 15 min, the kneading stage starts. During the kneading stage the power consumption drops rapidly (within 3 min) to 150 W and remains constant. During this period, also the pellet size distribution does not change which indicates a steady state.

3.4. Intragranular porosity

In order to characterise the pellets, mercury porosimetry was performed on three batches which were prepared in the Gral 10. The impeller speed during the kneading phase was set to 650 rpm to elucidate the effect of kneading on the porosity. The prepared batches were taken at $t = 5{:}15$ min (just before the end of the liquid addition), at $t = 7{:}25$ min (2 min kneading) and at $t = 20{:}25$ min (15 min kneading). The batches were sieved, so the differences in size could be investigated. Table 4 gives the porosity data. Although the amount of data is limited they give an indication of the effect of the kneading on the pellets. The porosity becomes lower after intense kneading. The larger pellets have a higher porosity compared with the smaller pellets. The smaller pellets are probably more susceptible to compression, while the larger pellets will be more susceptible to deformation and break-up.

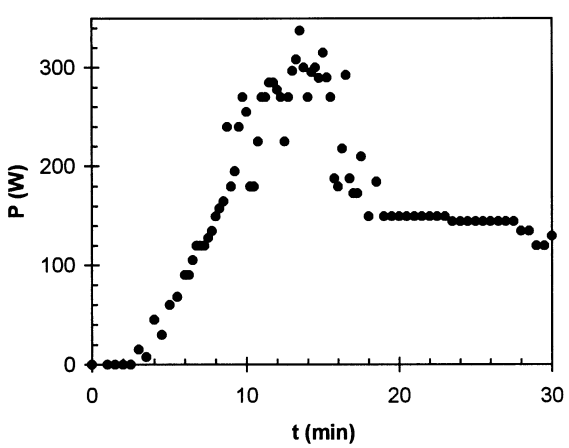

Fig. 4. The power consumption curve of the Gral 25.

Table 4
The porosity of the pellets as measured with mercury porosimetry

Time (min)	Size class (μm)	Porosity
5:15	200–500	0.117
7:25	200–500	0.062
20:25	850–1200	0.023
5:15	1250–1500	0.194
7:25	1250–1500	0.081
20:25	1250–1500	0.018

Final porosities are found less than 10% which is comparable with porosities found during melt pelletisation (Schæfer et al., 1993), and extrusion/spheronisation (Vervaet et al., 1995).

3.5. Definition of the growth mechanism

On the basis of the experiments we define the destructive nucleation growth mechanism (Fig. 5). The nucleation starts with one droplet. At the moment the droplet reaches the moving powder bed, a nucleus is formed. This nucleus is a loose agglomerate and can be characterised by a high porosity and a low tensile strength. The primary nucleus grow due to layering. The size of the primary nucleus is approximately 5 mm. Break-up of the nuclei proceeds according to two mechanisms: attrition and fragmentation. The weak nuclei wear off due to nuclei/nuclei and nuclei/wall collisions (attrition), and break into fragments because of the action of the impeller and chopper (fragmentation). Both mechanisms cause the formation of very small secondary nuclei. These secondary nuclei are the starting materials for the exponential growth. The exponential growth starts when the solid mass is sufficiently wetted and densification of the secondary nuclei occurs. Due to the densification stronger pellets are formed, which survive many collisions. Another consequence of the densification is that liquid is

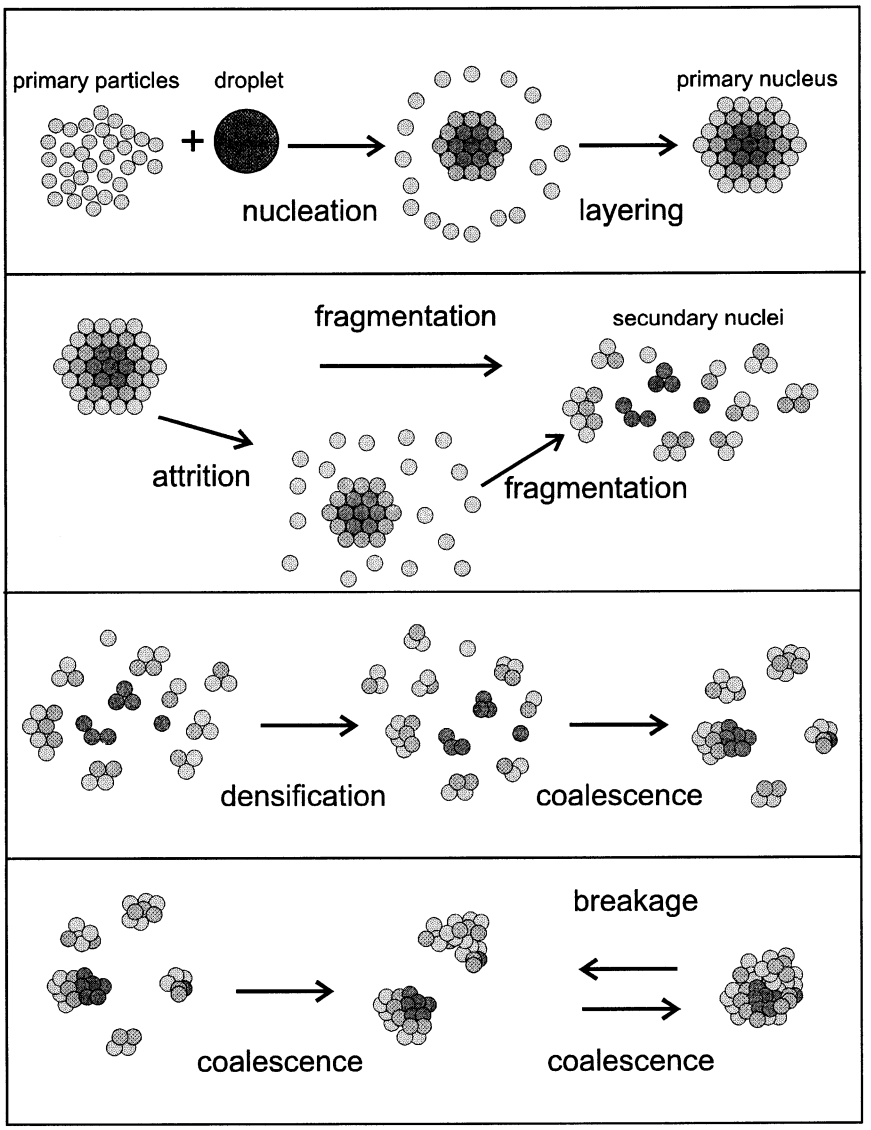

Fig. 5. The destructive nucleation growth mechanism of high-shear pelletisation.

squeezed to the pellet surface, which increases the coalescence probability. During kneading, coalescence proceeds because densification still occurs. The growth rate decreases because no more liquid is applied, and break-up becomes more and more important.

The proposed mechanism is not a step-wise process, but a combination of all different sub-mechanisms which occur at the same time. During liquid addition, the formation of primary and secondary nuclei is the major mechanism. However, the increasing d_{90} indicates growth due to densification at an early stage of the process. The importance of the different sub-mechanisms changes during the process. Densification of the pellets becomes more important during kneading, which leads to more spherical pellets with a lower porosity at a higher kneading time.

4. Conclusions

Like many other granulation processes, different phases of growth during high-shear pelletisation were identified: nucleation, fragmentation, densification, exponential growth due to coalescence, and break-up. The early stages of the pelletisation process was characterised by the formation of large primary nuclei from single droplets and fragmentation of the primary nuclei by the impeller and the chopper, forming small secondary nuclei. Growth started when the solid mass was sufficiently wetted and densification of the secondary nuclei occurred. During the final stages of the liquid addition phase exponential growth by coalescence was observed. Probably, the exponential growth rate depends linearly on the specific liquid addition rate and the impeller speed. During the kneading phase, pellets became more dense, and growth was diminished and seemed to be ended. The final pellet size was depending on the impeller speed and the liquid content. Because the pellet growth was ceased, good control of the final pellet size was possible. On the basis of the experiments, the destructive nucleation growth mechanism of high-shear pelletisation was designed identifying nucleation, fragmentation, densification, exponential growth by coalescence, and break-up.

5. List of symbols

a (m/s^2), acceleration; A (m^2), area; d (m), diameter; F (N), force; k (s^{-1}), growth coefficient; M, liquid content; P (W), power consumption; S, saturation; t (s), time; v (m/s), velocity; ϵ, porosity; γ_l (N/m), surface tension; ρ (kg/m^3), density; σ (Pa), tensile strength; θ (°), angle of contact.

References

Adetayo, A.A., Litster, J.D., Desai, M., 1993. The effect of process parameters on drum granulation of fertilizers with broad size distributions. Chem. Eng. Sci. 48, 3951–3961.

Adetayo, A.A., Litster, J.D., Pratsinis, S.E., Ennis, B.J., 1995. Population balance modelling of drum granulation of materials with wide size distribution. Powder Technol. 82, 37–49.

Carstensen, J.T., Lai, T., Flickner, D.W., Huber, H.E., Zoglio, M.A., 1976. Physical aspects of wet granulation I: Distribution kinetics of water. J. Pharm. Sci. 65, 992–997.

Ek, R., Alderborn, G., Nyström, C., 1994. Particle analysis of microcrystalline cellulose: Differentiation between individual particles and their agglomerates. Int. J. Pharm. 111, 43–50.

Ennis, B.J., 1996. Agglomeration and size enlargement. Session summary paper. Powder Technol. 88, 203–225.

Hancock, B.C., York, P., Rowe, R.C., 1992. Characterization of wet masses using a mixer torque rheometer: 2. mixing kinetics. Int. J. Pharm. 83, 147–153.

Holm, P., Jungersen, O., Schæfer, T., Kristensen, H.G., 1983. Granulation in high-speed mixers. Part I. Effects of process variables during kneading. Pharm. Ind. 45, 806–811.

Holm, P., Schæfer, T., Kristensen, H.G., 1985. Granulation in high-speed mixers. Part VI. Effects of process conditions on power consumption and granule growth. Powder Technol. 43, 225–233.

Holm, P., 1996. Pelletization by granulation in a roto-processor RP-2. Part I: Effects of process and product variables on granule growth. Pharm. Technol. Eur. 8, 22–36.

Hoornaert, F., Meesters, G., Pratsinis, S., Scarlett, B., 1994. Powder agglomeration in a Lödige granulator. In: Proceedings of the 1st International Particle Technology Forum, vol. 1, Denver, CO, pp. 278–283.

Kapur, P.C., Fuerstenau, D.W., 1966. Size distributions and kinetic relationships in the nuclei region of wet pelletization. Ind. Eng. Chem. Process Des. Dev. 5, 5–10.

Knight, P.C., 1993. An investigation of the kinetics of granulation using a high shear mixer. Powder Technol. 77, 159–169.

Kristensen, H.G., Schæfer, T., 1995. Growth kinetics of granulation in a high shear mixer. In: Proceedings of the 1st World Meeting APGI/APV, Budapest, pp. 151–152.

Leuenberger, H., Imanidis, G., 1986. Monitoring mass transfer processes to control moist agglomeration. Pharm. Technol. March, 56–73.

Newton, J.M., Chapman, S.R., Rowe, R.C., 1995. The influence of process variables on the preparation and properties of spherical granules by the process of extrusion and spheronisation. Int. J. Pharm. 120, 101–109.

Ouchiyama, N., Tanaka, T., 1975. The probability of coalescence in granulation kinetics. Ind. Eng. Chem. Process Des. Dev. 14, 286–289.

Potapov, A.V., Campbell, C.S., 1994. Computer simulation of impact-induced particle breakage. Powder Technol. 81, 207–216.

Sastry, K.V.S., Fürstenau, D.W., 1977. Kinetic and process analysis of the agglomeration of particulate materials of green pelletization. In: Sastry, K.V.S. (Ed.), Agglomeration 77. AIME, New York, pp. 381–402.

Schæfer, T., Holm, P., Kristensen, H.G., 1992. Melt pelletization in a high shear mixer. II. Power consumption and granule growth. Acta Pharm. Nordica. 4, 141–148.

Schæfer, T., Taagegaard, B., Thomsen, L.J., Kristensen, H.G., 1993. Melt pelletization in a high shear mixer. V. Effect of apparatus variables. Eur. J. Pharm. Sci. 1, 133–141.

Schæfer, T., Mathiesen, C., 1996. Melt pelletization in a high shear mixer. VIII. Effects of binder viscosity. Int. J. Pharm. 139, 125–138.

Schubert, H., Heidenreich, E., Neeße, T., 1990. Mechanische Verfahrenstechnik. Deutscher Verlag für Grundstoffindustrie, Leipzig.

Thornton, C., Yin, K.K., Adams, M.J., 1996. Numerical simulation of the impact fracture and fragmentation of agglomerates. J. Phys. D: Appl. Phys. 29, 424–435.

Vertommen, J., Kinget, R., 1996. The influence of five selected processing and formulation variables on the release of riboflavin from pellets produced in a rotary processor. S. T. P. Pharma Sci. 6, 335–340.

Vervaet, C., Baert, L., Remon, J.P., 1995. Extrusion-spheronisation. A literature review. Int. J. Pharm. 116, 131–146.

.